Decreased expression of lysophosphatidylcholine (16:0/OH) in high resolution imaging mass spectrometry independently predicts biochemical recurrence after surgical treatment for prostate cancer

Takayuki Goto[1)], Naoki Terada[1)], Takahiro Inoue[1)], Takashi Kobayashi[1)], Kenji Nakayama[1)], Yoshiyuki Okada[1)], Takeshi Yoshikawa[1)], Yu Miyazaki[1)], Masayuki Uegaki[1)], Noriaki Utsunomiya[1)], Yuki Makino[1)], Shinji Sumiyoshi[2)], Toshinari Yamasaki[1)], Tomomi Kamba[1)], Osamu Ogawa[1)]

1) Department of Urology, Graduate School of Medicine, Kyoto University, Kyoto, Japan

2) Department of Diagnostic Pathology, Kyoto University Hospital, Kyoto, Japan

Address correspondence to: Osamu Ogawa, M.D., Ph.D., Department of Urology, Graduate School of Medicine, Kyoto University, 54 Shogoin-Kawahara-Cho, Sakyo-Ku, Kyoto 606-8507, Japan

Tel: +81-75-751-3325; Fax: +81-75- 761-3441; E-mail: ogawao@kuhp.kyoto-u.ac.jp

Running head: Lysophosphatidylcholine and prostate cancer

Grant Support: This work was supported by a grant from the Japan Society for the Promotion of Science (JSPS) through the “Funding Program for World-Leading Innovative R&D on Science and Technology (FIRST Program),” initiated by the Council for Science and Technology Policy (CSTP) (http://www.first-ms3d.jp/english/).

Disclosure statement: The authors declare no competing financial interests.

Abstract

Background: Human prostate cancers are highly heterogeneous, indicating a need for various novel biomarkers to predict their prognosis. Lipid metabolism affects numerous cellular processes, including cell growth, proliferation, differentiation and motility. Direct profiling of lipids in tissue using high-resolution matrix-assisted laser desorption/ionization imaging mass spectrometry (HR-MALDI-IMS) may provide molecular details that supplement tissue morphology.

Methods: Prostate tissue samples were obtained from 31 patients with localized prostate cancer who underwent radical prostatectomy. The samples were assessed by HR-MALDI-IMS in positive mode, with the molecules identified by tandem mass spectrometry (MS/MS). The effect of identified molecules on prostate specific antigen recurrence free survival after radical prostatectomy was determined by Cox regression analysis and by the Kaplan–Meier method.

Results: Thirteen molecules were found to be highly expressed in prostate tissue, with five being significantly lower in cancer tissue than in benign epithelium. MS/MS showed that these molecules were [lysophosphatidylcholine (LPC)(16:0/OH)+H]$^+$, [LPC(16:0/OH)+Na]$^+$, [LPC(16:0/OH)+K]$^+$, [LPC(16:0/OH)+matrix+H]$^+$, and [sphingomyelin(SM)(d18:1/16:0)+H]$^+$. Reduced expression of LPC(16:0/OH) in cancer tissue was an independent predictor of biochemical recurrence after radical prostatectomy.

Conclusions: HR-MALDI-IMS showed that the expression of LPC(16:0/OH) and SM(d18:1/16:0) was lower in prostate cancer than in benign prostate epithelium. These differences in expression of phospholipids may predict prostate cancer aggressiveness, and provide new insights into lipid metabolism in prostate cancer.

Key words: imaging mass spectrometry, lysophosphatidylcholine, prostate cancer, biomarker, lipid

Introduction

Prostate cancer is one of the most common cancers and the major cause of cancer-related deaths in men, especially in Western countries [1]. Prostate specific antigen (PSA) is widely used to screen men diagnosed with prostate cancer and is regarded as a useful marker of disease recurrence subsequent to treatment. PSA, however, lacks specificity as a screening tool for prostate cancer, and there is no lower limit of PSA that entirely excludes cancer. In addition, although 20% to 30% of men experience PSA recurrence after radical prostatectomy, preoperative PSA does not correlate with cancer aggressiveness [2, 3]. Therefore, new specific biomarkers associated with cancer aggressiveness are needed to assist in the detection and treatment of prostate cancer.

Lipid metabolism plays an important role in human carcinogenesis by affecting numerous cellular processes, including cell growth, proliferation, differentiation and motility [4-6]. Many individual polar lipids, including lysophosphatidic acid (LPA) [7-12] , and cholesterol-like molecules [13, 14] have been associated with the development of prostate cancer. The expression patterns of several phospholipids have been reported to differ in prostate cancer and benign prostate tissue [15]. However, it has been difficult to measure the levels of expression of these molecules in prostate tissue, because the procedures used to measure for lipids, including conventional mass spectrometry (MS), require tissue extraction. This is especially problematic, because the lipids differ in spatial distribution within cells and tissues. An emerging tool, matrix assisted laser desorption/ionization imaging mass spectrometry (MALDI-IMS), can provide "*in situ* imaging", allowing the histological structures of bio-materials to be preserved and the mapped images compared with their corresponding histological images [16-18]. Prostate cancer is multifocal, with tumor areas surrounded by benign prostate epithelium and stroma, making it difficult to identify cancer specific regions by conventional

resolution MALDI-IMS. The spatial resolution of this technique was recently improved, to less than 10 μm, allowing a detailed two-dimensional analysis of phospholipids [19-24]. The 10 μm pitch of high-resolution matrix-assisted laser desorption/ionization imaging mass spectrometry (HR-MALDI-IMS) was shown sufficient to clearly visualize prostate cancer specific regions, enabling us to identify several phosphatidylinositols as being more highly expressed in prostate cancer than in benign prostate epithelium by HR-MALDI-IMS in negative mode [25].

This study utilized HR-MALDI-IMS analysis in positive mode to investigate the distribution of other lipids in prostate cancer tissue. This method enabled the identification of several phospholipids expressed to a lower extent in prostate cancer than in adjacent benign epithelium. Moreover, one of the identified phospholipids, lysophosphatidylcholine (LPC)(16:0/OH), was found to be a potential biomarker predictive of PSA recurrence after surgical treatment.

Materials and methods

Ethics Statement

All patients provided written informed consent for the use of their clinical samples. The study was approved by the institutional review board of Kyoto University Hospital.

Preparation of tissue samples

The patient cohort consisted of 31 Japanese males with clinically localized prostate cancer who underwent radical prostatectomy at Kyoto University Hospital from 2005 to 2008. Prostate tissue slices 5 mm thick were harvested immediately after removal and embedded in optimal cutting temperature (OCT) compound (Tissue-Tek®; Sakura Finetek, Torrance, CA, USA), without sucrose treatment to avoid the influence of fixation, and stored at –80°C. All frozen blocks yielded sections containing benign epithelium and cancer tissue.

Histological evaluation and matrix coating of prostate tissue samples

We previously established a protocol using HR-MALDI-IMS to analyze human prostate tissue samples embedded in OCT compound [25]. Samples were evaluated histologically and matrices were coated as described. The tissue samples were cryosectioned on a cryostat (CM1850; Leica, Wetzler, Germany) at –20°C, and cryosections 5 μm thick were mounted onto glass slides (MAS coat; Matsunami, Osaka, Japan) for hematoxylin and eosin (H&E) staining. All slides were evaluated by a single pathologist (S.S.) to determine tissue morphology and as a guide for HR-MALDI-IMS

analysis. Additional serial sections 10 μm thick were mounted onto indium-tin oxide–coated (ITO) glass slides (Sigma-Aldrich, St Louis, MO, USA) and used for HR-MALDI-IMS analysis. Each section was coated with 9-aminoacridine hemihydrates (9-AA) (Acros Organics, Geel, Belgium), which served as the matrix for MALDI-MS. Each slide was anchored in vacuum deposition equipment (SVC-700TM／700-2; Sanyu Electron, Tokyo, Japan) and coated with a 9-AA matrix layer obtained by sublimation at 220°C. The time required for vapor deposition was 8 min. The sections assessed by HR-MALDI-IMS were also stained with H&E and assessed by the pathologist. For H&E staining after HR-MALDI-IMS analysis, 9-AA was removed from the slides by dipping them in methanol for 30 s.

HR-MALDI-IMS and MS/MS analyses.

HR-MALDI-IMS analysis was performed on an atmospheric pressure MALDI-IT-TOF mass spectrometer (prototype Mass Microscope; Shimadzu, Kyoto, Japan), equipped with a 355-nm Nd: YAG laser. Mass spectrometry data were acquired in positive mode in the mass range of m/z 490–1000 using an external calibration method with mass resolving power 10,000 at m/z 1000. A region of interest (ROI) containing benign epithelium, cancer tissue and stroma was randomly determined from the microscopic view of each slide, and mass spectra were obtained at a spatial resolution of 10 μm. The ROIs were reconfirmed by analyzing the 10-μm thick samples stained with H&E after HR-MADLI-IMS. The same instrument was used for tandem mass spectrometry (MS/MS) analysis; the lipid class and fatty acid composition of the observed peaks were based on the spectral patterns of the ion peaks of the products. Results were compared with the Human Metabolome Database (http://www.hmdb.ca/), the Nature Lipidomics Gateway

(http://www.lipidmaps.org/) and published MS/MS data [26-30].

Data processing and statistical analysis of HR-MALDI-IMS results

Using SIMtools software (in-house software; Shimadzu Corporation, Kyoto, Japan), the mass profiles were normalized relative to the total ion current to eliminate variations in ionization efficiency, and the obtained normalized signal intensity was used for all imaging and statistical analyses. Ion images were visualized using Biomap software (Novartis, Basel, Switzerland). Mann–Whitney (M–W) U tests were used to compare factors between benign epithelium and cancer. The relationships among the expression of [lysophosphatidylcholine (LPC)(16:0/OH)+H]$^+$, [LPC(16:0/OH)+Na]$^+$, [LPC(16:0/OH)+K]$^+$ and [LPC(16:0/OH)+matrix+H]$^+$ were analyzed by the Spearman rank correlation. PSA recurrence was defined as a PSA level ≥0.2 ng/mL after surgery. Univariate and multivariate Cox regression analyses were used to analyze factors predicting PSA recurrence free survival after radical prostatectomy. The relationship between PSA recurrence free survival and LPC(16:0/OH) in cancer tissue was estimated by the Kaplan-Meier method and compared using the log rank test. Cutoffs used in Cox regression analysis and the Kaplan–Meier method including median age (65 years), median preoperative PSA level (7.3 ng/mL), and median levels of expression in cancer tissue of LPC(16:0/OH; signal intensity, 2126.4) and sphingomyelin(SM)(d18:1/16:0; signal intensity, 640.1). All statistical analyses were performed using JMP version 10.0.2 software (SAS Institute Japan Inc., Tokyo, Japan), with $p < 0.05$ considered statistically significant.

Results

Thirteen molecules were identified as highly expressed in human prostate tissues

Human prostate tissue samples embedded in OCT compound were analyzed by HR-MALDI-IMS in positive mode in the mass range of m/z 490–1000 (Figure 1A, B). The characteristics of the 31 included patients are shown in Table 1. ROIs containing benign epithelium, cancer tissue and stroma were randomly selected, and the top 50 peaks of the mass spectra were analyzed in each sample. After matrix and isotopic peaks had been excluded, 13 peaks were present in 25 or more of the 31 samples (Table S1). The ion images of these 13 molecules could be clearly visualized in prostate cancer and benign epithelium using HR-MALDI-IMS (Figure 1C).

The expression levels of 5 phospholipids were lower in cancer than in benign epithelium

A comparison of the signal intensities of these 13 molecules showed that the levels of expression of five of these molecules were significantly lower in cancer than in benign epithelium (Figure 1D, E, Table 2), with m/z measurements of 496.3, 518.3, 534.3, 690.4 and 703.5, respectively. The structures of these molecules were examined by MS/MS analyses of the peaks of their precursor ions (Figure S1, Table S2), showing that the molecules at m/z 496.3, 518.3, 534.3, 690.4 and 703.5 were [lysophosphatidylcholine (LPC) (16:0/OH)+H]$^+$, [LPC(16:0/OH)+Na]$^+$, [LPC(16:0/OH)+K]$^+$, [LPC(16:0/OH)+matrix+H]$^+$, and 703.5; [SM(d18:1/16:0)+H]$^+$, respectively. Representative visualizations of the distribution of these five molecules on HR-MALDI-IMS analyses indicated that their levels of expression were similarly lower in cancer compared with

benign epithelium (Figure 2).

LPC(16:0/OH) expression is a potentially independent biomarker predicting PSA recurrence

Four of the five molecules were LPC(16:0/OH) with various ion adducts, including Na, K and matrix. The levels of expression of $[LPC(16:0/OH)+H]^+$ in these samples strongly correlated with the levels of expression of $[LPC(16:0/OH)+Na]^+$ (R^2=0.813), $[LPC(16:0/OH)+K]^+$ (R^2=0.896), and $[LPC(16:0/OH)+matrix+H]^+$ (R^2=0.856; Figure 3A). Therefore, the level of expression of $[LPC(16:0/OH)+H]^+$ was considered representative of LPC(16:0/OH). The signal intensities of LPC(16:0/OH) and SM(d18:1/16:0) in cancer tissue did not correlate with preoperative PSA concentration, Gleason score or pathological stage (data not shown). To determine whether the levels of LPC(16:0/OH) and SM(d18:1/16:0) in cancer tissue predicted clinical outcomes, both were assessed, using univariate and multivariate Cox regression analyses, for the correlation with PSA recurrence free survival after radical prostatectomy. Univariate analysis showed that the level of expression of LPC(16:0/OH) was the only significant predictor of PSA recurrence (hazard ratio [HR] 0.294, 95% confidence interval [CI] 0.081–0.863, p = 0.025), a finding supported on multivariate analysis (HR 0.188, 95% CI 0.032–0.805, p = 0.023) (Table 3). Figure 3B shows Kaplan–Meier curves of the influence of LPC(16:0/OH) expression on PSA recurrence after radical prostatectomy. The 16 patients with low LPC(16:0/OH) expression (signal intensity < 2126.4) were at significantly higher risk of PSA recurrence than the 15 patients with high LPC(16:0/OH) expression (signal intensity > 2126.4; p=0.027, log rank test).

Discussion

This study showed that HR-MALDI-IMS had several methodological advantages compared with conventional lipidomic methods on cancer tissue [25]. Early stage prostate cancer is often multifocal, with tumor tissue surrounded by benign prostate epithelium and stroma, and no apparent tumor mass. Therefore, lower-resolution IMS was unable to precisely distinguish prostate cancer specific regions from benign epithelium [31-37]. High-resolution IMS may overcome this limitation and may be useful for analyzing heterogeneous tissues, such as prostate cancers.

Lipids are a diverse classes of molecules with critical functions in cellular energy storage, structure, and signaling. This study found that the levels of expression of SM(d18:1/16:0) and LPC(16:0/OH) were lower in prostate cancer tissue than in normal epithelium. Eicosanoids, the metabolic product of arachidonic acid, were thought to trigger the loss of SM via the activation of sphingomyelinase [38]. The arachidonic acid pathway has been shown to play a role in the development and progression of prostate cancer, consistent with our findings. In patients with thyroid papillary and colon cancer, however, the expression of SM(d18:1/16:0) on MALDI-IMS was higher in tumor and stromal regions than in normal regions [18, 39]. Because those studies used conventional resolution IMS, without clearly separating cancer specific and stromal regions, those results could not be directly compared with ours. However, the patterns of expression of SM(d18:1/16:0) may differ among tumor types.

LPC is a precursor of lysophosphatidic acid (LPA), a biogenic lipid involved in prostate cancer initiation and progression [10-12]. LPC is changed to LPA by an enzyme such as

lysophospholipase D (lysoPLD). To date, however, the expression of LPC had not been analyzed in prostate cancer tissue. We found that the expression of LPC(16:0/OH) was markedly lower in prostate cancer tissue than in normal epithelium, suggesting that the reduced expression of LPC(16:0/OH) in cancer tissue may predict PSA recurrence after radical prostatectomy. The demand for LPA in cancer tissue may trigger the loss of LPC(16:0/OH) from tissue via the activation of lysoPLD. LysoPLD expression has been reported much higher in prostate cancer tissue than in benign epithelium, with lysoPLD expression significantly correlated with probability of PSA recurrence after surgery [40]. Further research is needed to elucidate the association between LPA and LPC in prostate cancer.

The expression and fatty acid composition of LPC are also affected by *de novo* synthesis and remodeling pathway (Lands' pathway) [41, 42], with the diversity of fatty acids in LPC thought to be mainly affected by Lands' pathway. In the latter, LPC is produced by the hydrolysis of phosphatidylcholine (PC) by an enzyme such as phospholipase A2 (PLA2), and PC is produced by adduct of a fatty acid to LPC with lysophosphatidylcholine acyltransferases (LPCATs). The LPC(16:0/OH)/PC(16:0/18:1) ratio has been reported lower in hepatocellular carcinoma tissue, via the activation of LPCAT1, a key enzyme in the LPC remodeling pathway [43]. Moreover, increased expression of LPCAT1 correlated with the progression of prostate cancer [44-46], suggesting that increased expression of LPCAT1 may also reduce the expression of LPC(16:0/OH) in prostate cancer tissue. However, the expression of PC(16:0/18:1)(m/z760.5, 782.5, 798.5 and 954.6) was not significantly changed in our study. Therefore, the reduction in expression of LPC(16:0/OH) in prostate cancer tissue may be mainly due to the activity of lysoPLD rather than LPCAT1, at least in our clinical samples. Our study was preliminary and included a relatively limited number of samples.

Further studies are needed to determine whether changes in LPC(16:0/OH) expression and the activities of lysoPLD, PLA2 and LPCAT are correlated, and whether LPC(16:0/OH) is directly related to prostate cancer development.

Preoperative PSA, Gleason score, pathological stage and surgical margin are commonly indicators of risk of recurrence after treatment. Even in high risk patients, they have different prognostic value, indicating the need for markers to identify very high risk patients, for whom standard radical treatment has poor outcome and who would be suitable for clinical trials of more aggressive treatments, such as extended lymph node dissection or preoperative chemotherapy [47]. Our multivariate analysis showed that the reduced expression of LPC(16:0/OH) was a better predictor of PSA recurrence than other common indicators, including preoperative PSA, Gleason score, pathological stage and surgical margin.

The major limitations of our study included the small number of patients, with most having localized and well or moderately differentiated cancers. The expression of LPC(16:0/OH) should be verified in a larger cohort, including normal controls and patients with more aggressive disease. Moreover, the relationships between the expression of LPC(16:0/OH) and cancer specific survival remain to be determined.

Conclusions

HR-MALDI-IMS is a powerful tool to identify biomarkers in prostate cancer. The decreased expression of LPC(16:0/OH) is a potential biomarker of prostate cancer aggressiveness. Elucidation of mechanisms and verification of our findings in a larger patient cohort are needed.

Acknowledgments

We thank Koichi Tanaka and Taka-Aki Sato for help in performing the HR-MALDI-IMS experiments.

References

[1] Siegel R, Naishadham D, Jemal A: Cancer statistics, 2013. CA: a cancer journal for clinicians 2013, 63:11-30.

[2] Pound CR, Partin AW, Eisenberger MA, Chan DW, Pearson JD, Walsh PC: Natural history of progression after PSA elevation following radical prostatectomy. Jama 1999, 281:1591-7.

[3] Amling CL, Blute ML, Bergstralh EJ, Seay TM, Slezak J, Zincke H: Long-term hazard of progression after radical prostatectomy for clinically localized prostate cancer: continued risk of biochemical failure after 5 years. The Journal of urology 2000, 164:101-5.

[4] Santos CR, Schulze A: Lipid metabolism in cancer. The FEBS journal 2012, 279:2610-23.

[5] Menendez JA, Lupu R: Fatty acid synthase and the lipogenic phenotype in cancer pathogenesis. Nature reviews Cancer 2007, 7:763-77.

[6] Schulze A, Harris AL: How cancer metabolism is tuned for proliferation and vulnerable to disruption. Nature 2012, 491:364-73.

[7] Xie Y, Gibbs TC, Mukhin YV, Meier KE: Role for 18:1 lysophosphatidic acid as an autocrine mediator in prostate cancer cells. The Journal of biological chemistry 2002, 277:32516-26.

[8] Zeng Y, Kakehi Y, Nouh MA, Tsunemori H, Sugimoto M, Wu XX: Gene expression profiles of lysophosphatidic acid-related molecules in the prostate: relevance to prostate cancer and benign hyperplasia. The Prostate 2009, 69:283-92.

[9] Zhou X, Mao J, Ai J, Deng Y, Roth MR, Pound C, Henegar J, Welti R, Bigler SA: Identification of plasma lipid biomarkers for prostate cancer by lipidomics and bioinformatics. PloS one 2012, 7:e48889.

[10] Daaka Y: Mitogenic action of LPA in prostate. Biochimica et biophysica acta 2002, 1582:265-9.

[11] Terada N, Shiraishi T, Zeng Y, Mooney SM, Yeater DB, Mangold LA, Partin AW, Kulkarni P, Getzenberg RH: Cyr61 is regulated by cAMP-dependent protein kinase with serum levels correlating with prostate cancer aggressiveness. The Prostate 2012, 72:966-76.

[12] Kulkarni P, Getzenberg RH: High-fat diet, obesity and prostate disease: the ATX-LPA axis? Nature clinical practice Urology 2009, 6:128-31.

[13] Simons K, Ikonen E: Functional rafts in cell membranes. Nature 1997, 387:569-72.

[14] Zhuang L, Kim J, Adam RM, Solomon KR, Freeman MR: Cholesterol targeting alters lipid raft composition and cell survival in prostate cancer cells and xenografts. The Journal of clinical investigation 2005, 115:959-68.

[15] Rysman E, Brusselmans K, Scheys K, Timmermans L, Derua R, Munck S, Van Veldhoven PP, Waltregny D, Daniels VW, Machiels J, Vanderhoydonc F, Smans K, Waelkens E, Verhoeven G, Swinnen JV: De novo lipogenesis protects cancer cells from free radicals and chemotherapeutics by promoting membrane lipid saturation. Cancer research 2010, 70:8117-26.

[16] Schwamborn K, Caprioli RM: Molecular imaging by mass spectrometry--looking beyond classical histology. Nature reviews Cancer 2010, 10:639-46.

[17] Enomoto H, Sugiura Y, Setou M, Zaima N: Visualization of phosphatidylcholine, lysophosphatidylcholine and sphingomyelin in mouse tongue body by matrix-assisted laser desorption/ionization imaging mass spectrometry. Analytical and bioanalytical chemistry 2011, 400:1913-21.

[18] Ishikawa S, Tateya I, Hayasaka T, Masaki N, Takizawa Y, Ohno S, Kojima T, Kitani Y, Kitamura M, Hirano S, Setou M, Ito J: Increased expression of phosphatidylcholine (16:0/18:1) and (16:0/18:2) in thyroid papillary cancer. PloS one 2012, 7:e48873.

[19] Kubo A, Ohmura M, Wakui M, Harada T, Kajihara S, Ogawa K, Suemizu H, Nakamura M, Setou M, Suematsu M: Semi-quantitative analyses of metabolic systems of human colon cancer metastatic xenografts in livers of superimmunodeficient NOG mice. Analytical and bioanalytical chemistry 2011, 400:1895-904.

[20] Schober Y, Guenther S, Spengler B, Rompp A: Single cell matrix-assisted laser desorption/ionization mass spectrometry imaging. Analytical chemistry 2012, 84:6293-7.

[21] Miura D, Fujimura Y, Yamato M, Hyodo F, Utsumi H, Tachibana H, Wariishi H: Ultrahighly sensitive in situ metabolomic imaging for visualizing spatiotemporal metabolic behaviors. Analytical chemistry 2010, 82:9789-96.

[22] Yasunaga M, Furuta M, Ogata K, Koga Y, Yamamoto Y, Takigahira M, Matsumura Y: The significance of microscopic mass spectrometry with high resolution in the visualisation of drug distribution. Scientific reports 2013, 3:3050.

[23] Kawashima M, Iwamoto N, Kawaguchi-Sakita N, Sugimoto M, Ueno T, Mikami Y, Terasawa K, Sato TA, Tanaka K, Shimizu K, Toi M: High-resolution imaging mass spectrometry reveals detailed spatial distribution of phosphatidylinositols in human breast cancer. Cancer science 2013, 104:1372-9.

[24] Kurabe N, Hayasaka T, Ogawa M, Masaki N, Ide Y, Waki M, Nakamura T, Kurachi K, Kahyo T, Shinmura K, Midorikawa Y, Sugiyama Y, Setou M, Sugimura H: Accumulated phosphatidylcholine (16:0/16:1) in human colorectal cancer; possible involvement of LPCAT4. Cancer science 2013, 104:1295-302.

[25] Goto T, Terada N, Inoue T, Nakayama K, Okada Y, Yoshikawa T, Miyazaki Y, Uegaki M, Sumiyoshi S, Kobayashi T, Kamba T, Yoshimura K, Ogawa O: The expression profile of phosphatidylinositol in high spatial resolution imaging mass spectrometry as a potential biomarker for

prostate cancer. PloS one 2014, 9:e90242.

[26] Berry KA, Hankin JA, Barkley RM, Spraggins JM, Caprioli RM, Murphy RC: MALDI imaging of lipid biochemistry in tissues by mass spectrometry. Chemical reviews 2011, 111:6491-512.

[27] Hayasaka T, Goto-Inoue N, Zaima N, Kimura Y, Setou M: Organ-specific distributions of lysophosphatidylcholine and triacylglycerol in mouse embryo. Lipids 2009, 44:837-48.

[28] Hsu FF, Turk J: Structural determination of sphingomyelin by tandem mass spectrometry with electrospray ionization. Journal of the American Society for Mass Spectrometry 2000, 11:437-49.

[29] Koizumi S, Yamamoto S, Hayasaka T, Konishi Y, Yamaguchi-Okada M, Goto-Inoue N, Sugiura Y, Setou M, Namba H: Imaging mass spectrometry revealed the production of lyso-phosphatidylcholine in the injured ischemic rat brain. Neuroscience 2010, 168:219-25.

[30] Hayasaka T, Goto-Inoue N, Sugiura Y, Zaima N, Nakanishi H, Ohishi K, Nakanishi S, Naito T, Taguchi R, Setou M: Matrix-assisted laser desorption/ionization quadrupole ion trap time-of-flight (MALDI-QIT-TOF)-based imaging mass spectrometry reveals a layered distribution of phospholipid molecular species in the mouse retina. Rapid communications in mass spectrometry : RCM 2008, 22:3415-26.

[31] Eberlin LS, Dill AL, Costa AB, Ifa DR, Cheng L, Masterson T, Koch M, Ratliff TL, Cooks RG: Cholesterol sulfate imaging in human prostate cancer tissue by desorption electrospray ionization mass spectrometry. Analytical chemistry 2010, 82:3430-4.

[32] Cazares LH, Troyer D, Mendrinos S, Lance RA, Nyalwidhe JO, Beydoun HA, Clements MA, Drake RR, Semmes OJ: Imaging mass spectrometry of a specific fragment of mitogen-activated protein kinase/extracellular signal-regulated kinase kinase kinase 2 discriminates cancer from uninvolved prostate tissue. Clinical cancer research : an official journal of the American Association for Cancer Research

2009, 15:5541-51.

[33] Schwamborn K, Krieg RC, Reska M, Jakse G, Knuechel R, Wellmann A: Identifying prostate carcinoma by MALDI-Imaging. International journal of molecular medicine 2007, 20:155-9.

[34] Bonnel D, Longuespee R, Franck J, Roudbaraki M, Gosset P, Day R, Salzet M, Fournier I: Multivariate analyses for biomarkers hunting and validation through on-tissue bottom-up or in-source decay in MALDI-MSI: application to prostate cancer. Analytical and bioanalytical chemistry 2011, 401:149-65.

[35] Pallua JD, Schaefer G, Seifarth C, Becker M, Meding S, Rauser S, Walch A, Handler M, Netzer M, Popovscaia M, Osl M, Baumgartner C, Lindner H, Kremser L, Sarg B, Bartsch G, Huck CW, Bonn GK, Klocker H: MALDI-MS tissue imaging identification of biliverdin reductase B overexpression in prostate cancer. Journal of proteomics 2013, 91C:500-14.

[36] Pirro V, Eberlin LS, Oliveri P, Cooks RG: Interactive hyperspectral approach for exploring and interpreting DESI-MS images of cancerous and normal tissue sections. The Analyst 2012, 137:2374-80.

[37] Steurer S, Borkowski C, Odinga S, Buchholz M, Koop C, Huland H, Becker M, Witt M, Trede D, Omidi M, Kraus O, Bahar AS, Seddiqi AS, Singer JM, Kwiatkowski M, Trusch M, Simon R, Wurlitzer M, Minner S, Schlomm T, Sauter G, Schluter H: MALDI mass spectrometric imaging based identification of clinically relevant signals in prostate cancer using large-scale tissue microarrays. International journal of cancer Journal international du cancer 2013, 133:920-8.

[38] Rao AM, Hatcher JF, Dempsey RJ: Lipid alterations in transient forebrain ischemia: possible new mechanisms of CDP-choline neuroprotection. Journal of neurochemistry 2000, 75:2528-35.

[39] Shimma S, Sugiura Y, Hayasaka T, Hoshikawa Y, Noda T, Setou M: MALDI-based imaging mass spectrometry revealed abnormal distribution of phospholipids in colon cancer liver metastasis. Journal of

chromatography B, Analytical technologies in the biomedical and life sciences 2007, 855:98-103.

[40] Nouh MA, Wu XX, Okazoe H, Tsunemori H, Haba R, Abou-Zeid AM, Saleem MD, Inui M, Sugimoto M, Aoki J, Kakehi Y: Expression of autotaxin and acylglycerol kinase in prostate cancer: association with cancer development and progression. Cancer science 2009, 100:1631-8.

[41] Kennedy EP, Weiss SB: The function of cytidine coenzymes in the biosynthesis of phospholipides. The Journal of biological chemistry 1956, 222:193-214.

[42] Lands WE: Metabolism of glycerolipides; a comparison of lecithin and triglyceride synthesis. The Journal of biological chemistry 1958, 231:883-8.

[43] Morita Y, Sakaguchi T, Ikegami K, Goto-Inoue N, Hayasaka T, Hang VT, Tanaka H, Harada T, Shibasaki Y, Suzuki A, Fukumoto K, Inaba K, Murakami M, Setou M, Konno H: Lysophosphatidylcholine acyltransferase 1 altered phospholipid composition and regulated hepatoma progression. Journal of hepatology 2013, 59:292-9.

[44] Grupp K, Sanader S, Sirma H, Simon R, Koop C, Prien K, Hube-Magg C, Salomon G, Graefen M, Heinzer H, Minner S, Izbicki JR, Sauter G, Schlomm T, Tsourlakis MC: High lysophosphatidylcholine acyltransferase 1 expression independently predicts high risk for biochemical recurrence in prostate cancers. Molecular oncology 2013, 7:1001-11.

[45] Zhou X, Lawrence TJ, He Z, Pound CR, Mao J, Bigler SA: The expression level of lysophosphatidylcholine acyltransferase 1 (LPCAT1) correlates to the progression of prostate cancer. Experimental and molecular pathology 2012, 92:105-10.

[46] Faas FH, Dang AQ, White J, Schaefer R, Johnson D: Increased prostatic lysophosphatidylcholine acyltransferase activity in human prostate cancer: a marker for malignancy. The Journal of urology 2001, 165:463-8.

[47] Vergis R, Corbishley CM, Norman AR, Bartlett J, Jhavar S, Borre M, Heeboll S, Horwich A, Huddart R, Khoo V, Eeles R, Cooper C, Sydes M, Dearnaley D, Parker C: Intrinsic markers of tumour hypoxia and angiogenesis in localised prostate cancer and outcome of radical treatment: a retrospective analysis of two randomised radiotherapy trials and one surgical cohort study. The Lancet Oncology 2008, 9:342-51.

Figure Legends

Figure 1.

Direct tissue mass spectrometric analysis of human prostate tissue (Patient 1).

Matrix coated tissue was assessed by positive ion mode HR-MALDI-IMS in the mass range of m/z 490–1000.

A, Hematoxylin and eosin (H&E) stained human prostate tissue specimen containing defined areas of benign epithelium (blue) and prostate cancer (red). The scale bar represents 200 μm.

B, D and E, Regions of interest and resulting averaged mass of benign epithelium, cancer tissue and stroma containing region (B; green), benign epithelium specific region (D; blue), and prostate cancer specific region (E; red). The x- and y-axes shows m/z and signal intensity normalized to total ion current, respectively.

C, Mass spectrometry image showing the distribution of 13 common molecules.

Figure 2.

Visualization of molecular distribution of 5 molecules lowly expressed in cancer tissue.

H&E stained and mass spectrometry images of samples from 6 patients. H&E stained images show defined areas of benign epithelium (blue) and prostate cancer (red). The scale bar represents 200 μm. Mass spectrometry images show the representative distribution of [lysophosphatidylcholine (LPC)(16:0/OH)+H]$^+$, [LPC(16:0/OH)+Na]$^+$, [LPC(16:0/OH)+K]$^+$, [LPC(16:0/OH)+matrix+H]$^+$, and [sphingomyelin (SM)(d18:1/16:0)+H]$^+$, which were expressed to a lower extent in cancer than in benign epithelium.

Figure 3.

Statistical analyses of the expression of LPC(16:0/OH) in cancer tissue.

A, The relationship between the signal intensity of $[LPC(16:0/OH)+H]^+$ and the signal intensities of $[LPC(16:0/OH)+Na]^+$, $[LPC(16:0/OH)+K]^+$, and $[LPC(16:0/OH)+matrix+H]^+$.

B, Kaplan–Meier curves show the relationship between LPC(16:0/OH) expression and PSA recurrence free survival. The median level of expression of LPC(16:0/OH) in cancer tissue (signal intensity: 2126.4) served as cut off for high vs low expression.

Figure 1.

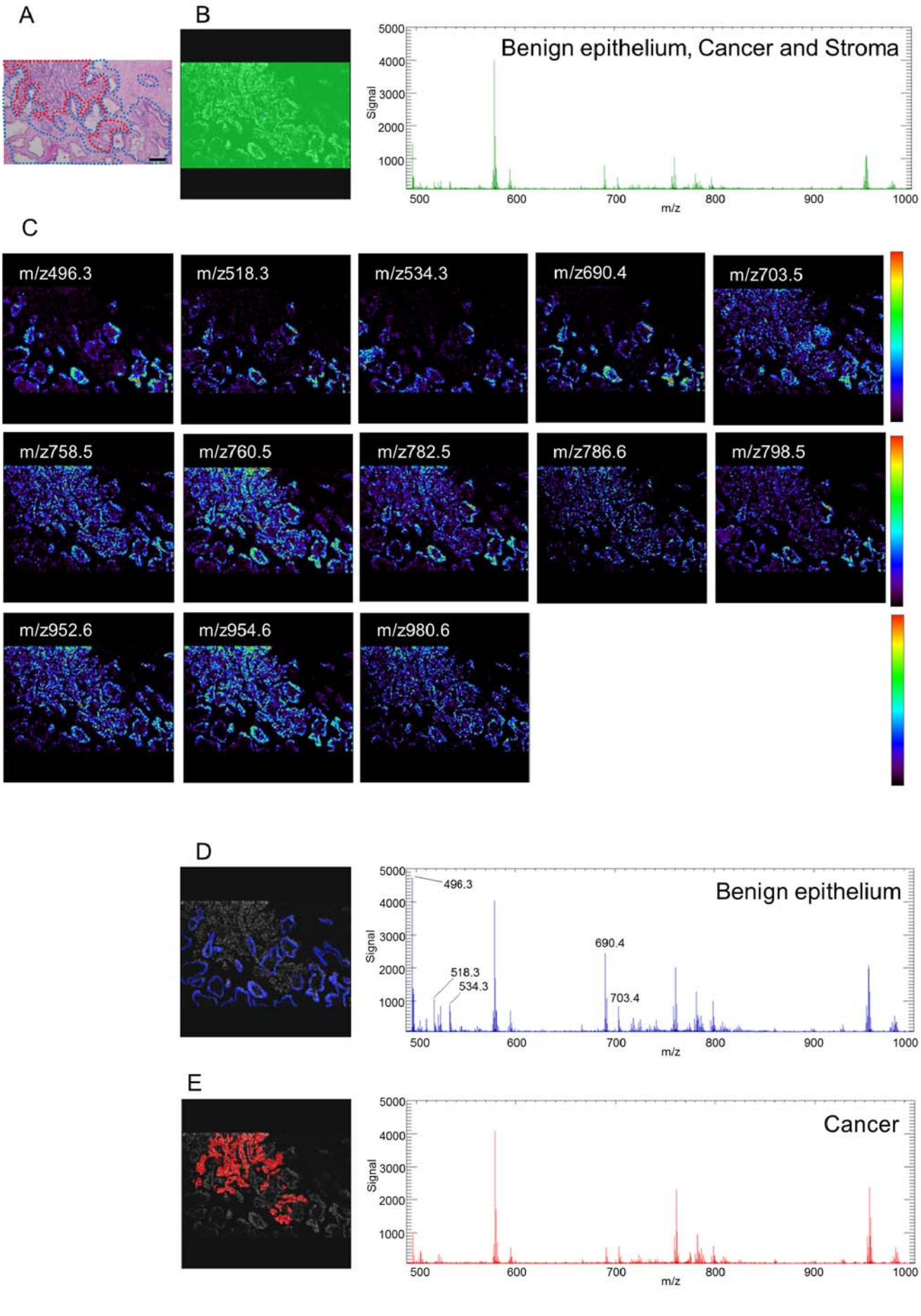
A
B
Benign epithelium, Cancer and Stroma
Signal
m/z
C
m/z496.3
m/z518.3
m/z534.3
m/z690.4
m/z703.5
m/z758.5
m/z760.5
m/z782.5
m/z786.6
m/z798.5
m/z952.6
m/z954.6
m/z980.6
D
Benign epithelium
496.3
518.3
534.3
690.4
703.4
E
Cancer

Figure 2.

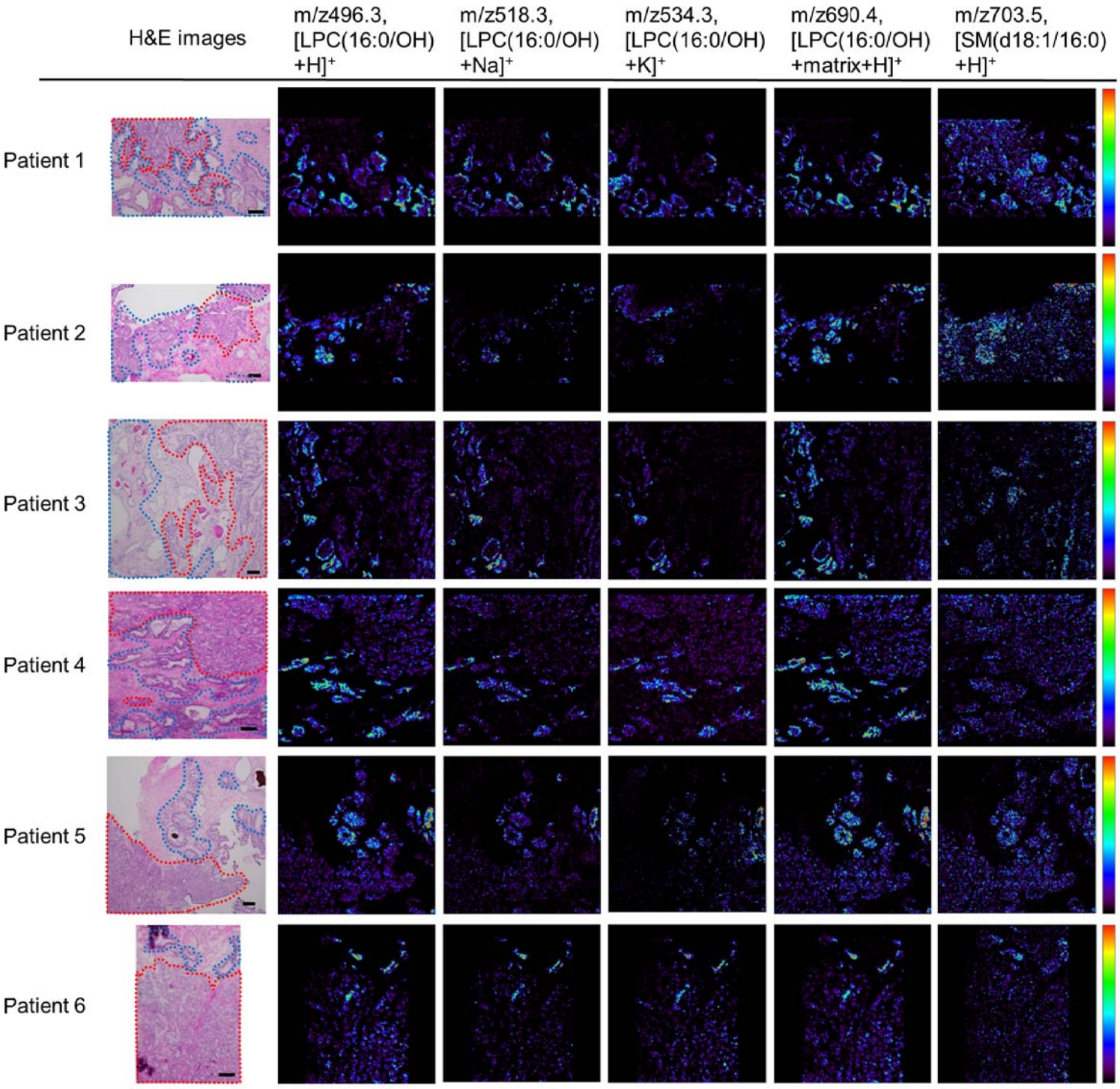
H&E images
m/z496.3, [LPC(16:0/OH) +H]+
m/z518.3, [LPC(16:0/OH) +Na]+
m/z534.3, [LPC(16:0/OH) +K]+
m/z690.4, [LPC(16:0/OH) +matrix+H]+
m/z703.5, [SM(d18:1/16:0) +H]+
Patient 1
Patient 2
Patient 3
Patient 4
Patient 5
Patient 6

Figure 3.

A

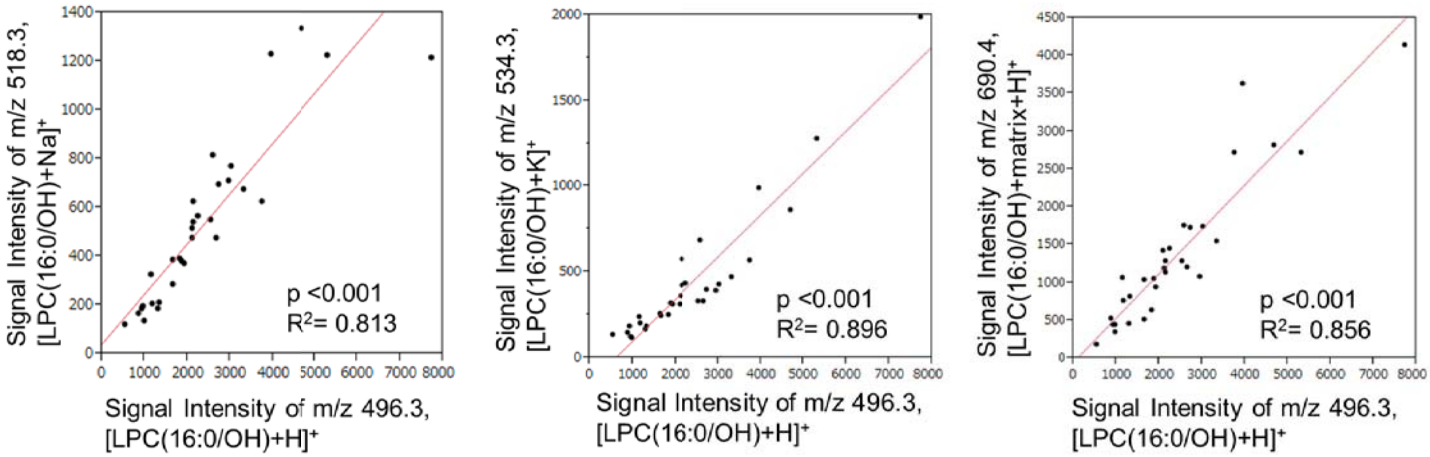

B

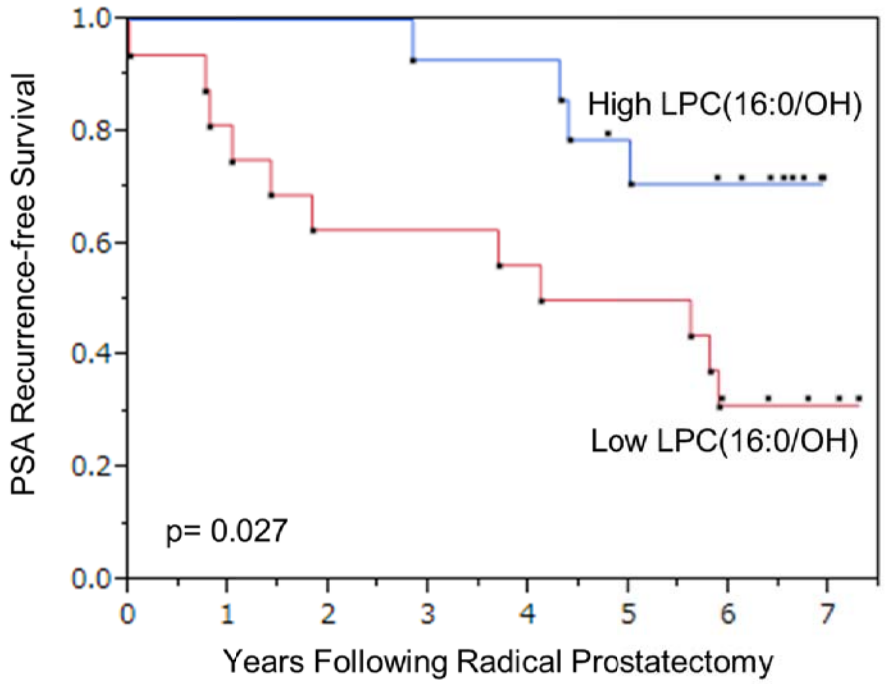

Number at risk

High	15	15	15	14	14	11	9	0
Low	16	14	11	11	10	9	5	3

Table1. Clinical and pathological characteristics of the 31 patients resected for prostate cancer.

Category	Subcategory	Total
Number of patients		31
Mean ± SD age, yr		64.7 ± 7.4
Mean ± SD preoperative PSA, ng/mL		8.85 ± 4.68
Mean ± SD prostate weight, g		38.6 ± 12.0
Gleason scores, n (%)		
	6	11 (35)
	7	14 (45)
	8	5 (16)
	9	1 (3)
Pathological stage, n (%)		
	pT2a	2 (6)
	pT2c	21 (68)
	pT3a	6 (19)
	pT3b	2 (6)
Surgical margins, n (%)		
	Negative	17 (55)
	Positive	14 (45)
PSA recurrence, n (%)		
	+	15 (48)
	-	16 (52)

Abbreviations: SD, standard deviation. PSA, prostate specific antigen.

Table 2. Averaged signal intensities of common 13 molecules.

	m/z	Benign epithelium, n=31		Cancer, n=31		p*
		Mean	SD	Mean	SD	Value
A	m/z496.3	4979.2	2351.8	2394.8	1503.4	<0.001
B	m/z518.3	1270.2	770.4	535.0	343.4	<0.001
C	m/z534.3	1039.2	689.0	441.5	389.8	<0.001
D	m/z690.4	2611.6	1567.1	1354.9	954.5	<0.001
E	m/z703.5	918.8	463.2	656.7	268.0	0.025
F	m/z758.5	809.7	300.6	876.0	503.7	0.961
G	m/z760.5	2372.6	990.3	2843.6	1474.8	0.123
H	m/z782.5	1542.6	824.9	1420.0	747.1	0.751
I	m/z786.6	596.9	231.9	660.8	365.4	0.598
J	m/z798.5	1167.4	597.1	1022.8	461.7	0.531
K	m/z952.6	849.6	370.2	910.1	554.3	0.961
L	m/z954.6	2665.8	1032.4	3209.7	1756.6	0.301
M	m/z980.6	670.1	252.9	732.9	419.9	0.559

Abbreviations: SD, standard deviation. *Mann-Whitney U test

Table 3. Univariate and multivariate Cox regression analyses of pathologic parameters and phospholipid expression associated with PSA recurrence after radical prostatectomy.

	PSA recurrence		PSA recurrence		Univariate			Multivariate		
Category※	**(-)**		**(+)**		**HR (95% CI)**		**p value**	**HR (95% CI)**		**p value**
Number of patients	16		15							
Age, n(%)										
≦65yr	8	(50)	8	(53)	0.931	(0.326-2.596)	0.891	0.598	(0.183-1.975)	0.391
>65yr	8	(50)	7	(47)						
Preoperative PSA level, n(%)										
Low	9	(56)	7	(47)	1.335	(0.479-3.813)	0.576	1.415	(0.340-5.735)	0.624
High	7	(44)	8	(53)						
Gleason scores, n (%)										
≦7	13	(81)	12	(80)	0.864	(0.196-2.739)	0.820	0.281	(0.045-1.385)	0.123
>7	3	(19)	3	(20)						
Pathological stage, n (%)										
pT2	11	(69)	12	(80)	0.686	(0.156-2.166)	0.546	0.473	(0.082-2.018)	0.324
pT3	5	(31)	3	(20)						
Surgical margin, n (%)										
Negative	10	(63)	7	(47)	1.701	(0.607-4.879)	0.308	2.209	(0.544-8.741)	0.262
Positive	6	(38)	8	(53)						
Level of expression of										

LPC(16:0/OH), n(%)										
Low	5	(31)	11	(73)	0.294	(0.081-0.864)	0.025	0.188	(0.032-0.805)	0.023
High	11	(69)	4	(27)						
Level of expression of SM(d18:1/16:0), n(%)										
Low	6	(38)	10	(67)	0.393	(0.122-1.116)	0.080	0.793	(0.181-3.887)	0.762
High	10	(63)	5	(33)						

Abbreviations: PSA, prostate specific antigen. LPC, lysophosphatidylcholine. SM, sphingmyelin. HR, hazard ratio. CI, confidential interval.

※Median age (65 years old), median preoperative PSA level (7.3 ng/mL), and median levels of expression in cancer tissue of LPC(16:0/OH) (signal intensity: 2126.4) and SM(d18:1/16:0) (signal intensity: 2641.5) were used as cut off.